https://doi.org/10.3311/PPci.21784

Periodica Polytechnica Civil Engineering, 67(3), pp. 867–874, 2023

A Novel Higher-Order Zigzag Function Applied to Refined Unified Beam Theory for the Analysis of Composite Laminated Materials

Leonardo Fellipe Prado Leite[1], Fabio Carlos da Rocha[1*]

[1] Department of Civil Engineering, Laboratory of Building Materials and Structures (LAMCE), Federal University of Sergipe (UFS), 49100-000, São Cristóvão, Brazil
[*] Corresponding author, e-mail: fabiocrocha@academico.ufs.br

Received: 02 January 2023, Accepted: 20 April 2023, Published online: 08 May 2023

Abstract

Highly efficient materials and structures are becoming increasingly common in military, aeronautical, aerospace, mechanical, and civil engineering applications. Composite materials have been developed to address the need to combine two or more materials to achieve superior properties. Many structural elements, such as laminated beams, use composite materials, but an accurate mathematical model of the bending behavior is required due to the abrupt changes in material properties in the interlaminar zones. This accurate model can be achieved using zigzag theory. This theory is one of the most commonly used formulations for modeling laminated beams. This theory is an improvement of the equivalent single-layer theory as an additional term called the "zigzag function" is used to represent the variation in the axial displacement along the cross section. This paper proposes a novel high-order zigzag function in a sinusoidal format. Several higher-order beam theories are combined with the proposed functions, and their performances are compared with those of other functions in the literature. The results reveal excellent agreement between the proposed formulation and the reference solution as well as a more effective combination of zigzag functions and beam theory.

Keywords

composite materials, high-order beam theory, zigzag theory

1 Introduction

Several theories describe the structural behavior of beams, among which the best-known and most straightforward theory is the classical Euler–Bernoulli theory (EBT) [1]. Owing to the inability of EBT to account for shear strain, it is better suited for beams with a low height-to-length ratio.

To avoid this limitation of EBT, the first-order shear theory, also known as Timoshenko's beam theory (TBT) [2], was developed. Although TBT accounts for the shear effect, it still has the following drawbacks: the shear stresses at the top and bottom of the beam are not nulled; the warping effect of the cross section is not considered; the distribution of the shear stress field in the cross section is represented incorrectly; and correction factors need to be used. To overcome these drawbacks, theories for new higher-order kinematics, known as "high-order beam theories", have been proposed [3–8].

Single-material beams are frequently analyzed using high-order kinematics. However, composite materials have been developed, which provide greater flexibility in constructing new structures that are more efficient in the desired properties and thus provide greater diversity in applications in various fields [9]. Therefore, to improve the analysis of laminated composite beams, it is necessary to couple new parameters with the kinematics to capture the interactions between the laminae and the individual behavior of each lamina [9]. The main theories used in the analysis of laminated composite beams are the equivalent single-layer (ESL) theory, layerwise (LW) theory, and zigzag (ZZ) theory.

The LW and ZZ theories are more accurate than the ESL theory because they consider the behavior of each lamina separately. The LW theory yields results with good precision. However, it has unknown quantities proportional to the number of layers of the laminae, resulting in high computational costs. Thus, to decouple the number of unknowns in the problem from the number of layers without significant losses in the precision of the results, the ZZ approach was developed, which incorporates the ZZ effect into ESL theories [10].

Cite this article as: Prado Leite L. F., da Rocha, F. C. "A Novel Higher-Order Zigzag Function Applied to Refined Unified Beam Theory for the Analysis of Composite Laminated Materials", Periodica Polytechnica Civil Engineering, 67(3), pp. 867–874, 2023. https://doi.org/10.3311/PPci.21784

Several studies on ZZ laminated beam theory have been conducted. Murakami et al. [11] developed a function called the "zigzag", which only contains geometric information, and applied it to TBT. Di Sciuva [12, 13] formulated the ZZ theory with a Heaviside function and incorporated a cubic parcel into kinematic for plate problems. Tessler et al. [14] developed the refined ZZ theory (RZT) to aid in determining the stress fields for the TBT. Lularon et al. [15] studied the RZT and other beam theories, examining the buckling and bending behavior. They demonstrated the possibility of visualizing the difference between the stress fields calculated using equilibrium equations and constitutive relationships.

The Murakami ZZ function [11] was developed to provide more accurate formulations while maintaining simplicity. In the work of Carrera [16], the application of the Murakami format was studied in the static and dynamic analyses of plates. Accordingly, Carrera and Ciuffreda [17] developed a unified formulation for this problem. Vidal and Polit [18] showed the results of coupling between Murakami's ZZ function and sinusoidal higher-order beam kinematics. This combination enhances the precision of the displacement and stress field results.

This paper presents a unified formulation for higher-order kinematics that incorporates a new higher-order ZZ function in a sinusoidal format. Therefore, unlike in previous research [18], the beam theory and ZZ function are of a higher order.

The structure of the present paper is given as follows. Section 2 presents definitions, kinematics, governing equations and procedure for the analytical solution. In Section 3 provides a numerical example to validate the accuracy and performance of the proposed model for a laminated composite beam. In section 4, the concluding remarks are made.

2 Mathematical development

2.1 Definitions

A laminated composite beam with length $L = x_b - x_a$, subjected to load $q(x)$ and external forces T in the x- and z-directions, is considered, as shown in Fig. 1.

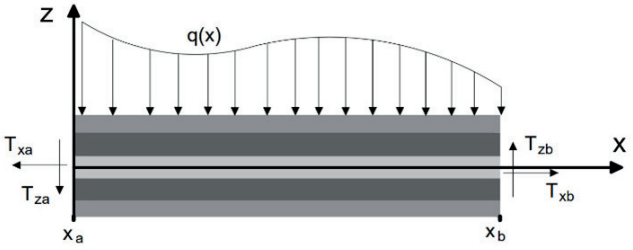

Fig. 1 General loading and geometry of a composite laminated beam

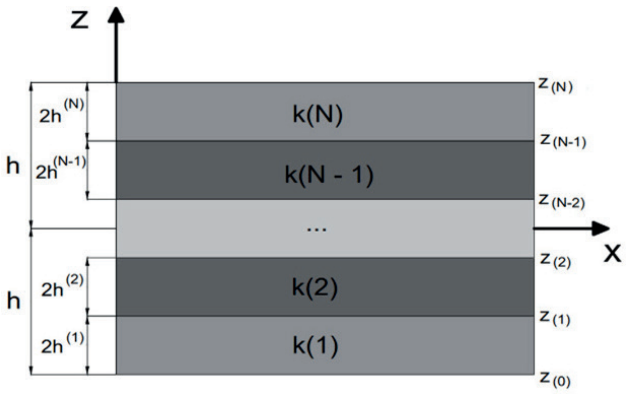

Fig. 2 General cross section and layers of a composite laminated beam

The cross-sectional height is denoted by $2h$, and the thickness of each lamina is identified by $2h^{(k)}$, where $k = 1, 2, ..., N$ represents layer numbering (Fig. 2). The global coordinates of the beam are given by $z_{(i)} (i = 0, 1, ..., N)$, $z_0 = -h$, $z_{N+1} = h$, and $z_{(i)} = z_{(i-1)} + 2h$ for $(i = 1, ..., N)$.

2.2 Kinematics

The present formulation is limited to the linear elastic behavior of the material. The displacement fields of various beam theories that consider shear deformation are chosen and unified based on the following hypotheses: (1) transverse deformation is absent, (2) the bending component of the axial displacement is similar to that given by classical beam theory, (3) the shear component of the axial displacement provides for the higher-order variation in stress and strain such that these response fields are zero on the upper and lower surfaces of the beam, and (4) the ZZ function is added, providing the zigzag behavior to the axial displacement of the laminated composite. Based on these hypotheses, the displacement fields for various theories of unified beams, considering high-order shear strain and the ZZ function, are given by Eq. (1) as follows:

$$\begin{aligned} u^{(k)}(x,z) &= u_0(x) - z w_0'(x) + f(z)\phi(x) + \phi_{zz}^{(k)}(z)\psi(x), \\ w(x,z) &= w_0(x), \end{aligned} \tag{1}$$

where $w(x)$ and $u^{(k)}(x, z)$ are the transverse and axial displacements of each layer, respectively, $w_0(x)$ and $u_0(x)$ are the transverse and axial displacements in the midplane of the beam, respectively $f(z)$, is a shape function that represents the higher-order stress and shear strain distribution along the beam depth (see Table 1), $\phi(x)$ is the angle resulting from shear, $\phi_{zz}^{(k)}$ is a ZZ function, and $\psi(x)$ is a ZZ amplitude function. Equation (1) can be written as a linearly elastic strain field given by Eq. (2) as follows:

$$\varepsilon^{(k)}(x,z)=\frac{du^{(k)}(x,z)}{dx}$$
$$=u_0{}'(x)-zw_0''(x)+f(z)\phi'(x)+\phi_{zz}^{(k)}(z)\psi'(x),$$
$$\gamma^{(k)}(x,z)=\frac{dw(x)}{dx}+\frac{du^{(k)}(x,z)}{dx}=f'(z)\phi(x)+\beta(z)\psi(x), \quad (2)$$

where $\beta(z)$ is the first derivative of the ZZ function. The linear constitutive relationship for the beam can be written as

$$\sigma^{(k)}(x,z)=\overline{Q_{11}^{(k)}}\varepsilon^{(k)}(x,z),$$
$$\tau^{(k)}(x,z)=\overline{Q_{55}^{(k)}}\gamma^{(k)}(x,z), \quad (3)$$

where $\overline{Q_{11}^{(k)}}$ and $\overline{Q_{55}^{(k)}}$ are the elastic properties of orthotropic materials described in [9].

This study proposes a novel formulation for the higher-order ZZ function, $\phi_{zz}^{(k)}$, called "sinusoidal zigzag" (ZZ-SIN) (see Table 2). In addition, it is proposed to combine the proposed higher-order ZZ function (ZZ-SIN) with several other higher-order beam theories (see Table 1). ZZ-SIN was constructed from the function proposed by Murakami et al. [11] and is given by $\phi_{zz-MUR}^{(k)}(z)=(-1^{(k)})-[-2z+(z^{(k)}+z^{(k-1)})]/2h^{(k)}$. This proposal aims to improve the order of accuracy concerning linear ZZ functions that use higher-order beam theories, as in Vidal and Polit's work [18], which combines Murakami's ZZ function with the higher-order Touratier beam approach [5] (see Table 1).

2.3 Governing equations

The principle of virtual work (PVW) is used to develop the governing equations. The internal work of the beam is expressed as

$$\delta W_{int}=\int_V\left(\sigma^{(k)}\delta\varepsilon^{(k)}+\tau^{(k)}\delta\gamma^{(k)}\right)dV\ . \quad (4)$$

The external work performed, as shown in Fig. 1, is given by

$$\delta W_{ext}=\int_L q(x)\delta w_0(x)dx$$
$$+\int_A\left[T_{x_a}(x_a)\delta u^{(k)}(x_a,z)+T_{z_a}(z)\delta w_0(x_a)\right]dA \quad (5)$$
$$-\int_A\left[T_{x_b}(x_b)\delta u^{(k)}(x_b,z)+T_{z_b}(z)\delta w_0(x_b)\right]dA,$$

where $T_{x_\Delta}=T_x(x_\Delta,z)$, $T_{z_\Delta}=T_z(x_\Delta,z)$ (with Δ or b) are tractions, A is the cross-section area, L is the length, V is volume of the beam, and $q(x)$ is a loading function.

Table 1 Shape functions for unified high-order beam theory

Model	$f(z)$
KRU49 [3]	$\frac{5z}{4}\left(1-\frac{4z^2}{12h^2}\right)$
RED90 [4]	$z\left(1-\frac{4z^2}{12h^2}\right)$
TOU91 [5]	$\frac{2h}{\pi}\sin\left(\frac{\pi z}{2h}\right)$
SOL92 [6]	$z\cosh\left(\frac{1}{2}\right)-2h\sinh\left(\frac{z}{2h}\right)$
KAR03 [7]	$z\exp\left[-2\left(\frac{z}{2h}\right)^2\right]$
AKA07 [8]	$\frac{3\pi}{2}\left[2h\tanh\left(\frac{z}{2h}\right)-z\sec^2h\left(\frac{1}{2}\right)\right]$

Table 2 Zigzag functionsw

$\phi_{zz}^{(k)}(z)$ SIN-ZZ [Present]
$Sin\left[\phi_{MURzz}^{(k)}(z)\right]-\left[\left(\frac{z^2}{2z_0}\right)+\left(\frac{2z^3-3z_0z^2}{12z_N^2}\right)\right]\frac{d\phi_{MURzz}^{(0)}(z)}{dz}$ $-\left[\frac{2z^3-3z_0z^2}{12z_N^2}\right]\frac{d\phi_{MURzz}^{(N)}(z)}{dz}$

The functional for the problem is obtained through the PVW ($\delta_{Wint}=\delta_{Wext}$) and Eqs. (1)–(3), with variables field $u_0(x)$, $w(x)$, $w'(x)$, $\phi(x)$ and $\psi(x)$. The Euler equation is obtained from the first variation of the functional, Eq. (6), together with its boundary conditions shown in Eq. (7). Boundary variables with a slash above it identify as prescribed values.

$$Au_0''(x)-A_zw'''(x)+B\phi''(x)+D\psi''(x)=0,$$
$$A_zu_0'''(x)-A_{zz}w'''{}'(x)+B_z\phi'''^{(x)}+D_z\psi'''^{(x)}=q(x),$$
$$Bu_0''(x)-B_zw'''(x)+B_f\phi''(x)+D_f\psi''(x)=G_f\phi(x)+G\psi(x),$$
$$Du_0''(x)-D_zw'''(x)+D_f\phi''(x)+D_\phi\psi''^{(x)}=G\phi(x)+G_\beta\psi(x). \quad (6)$$

$$N_x(x_\Delta,z)=\overline{N_x}(x_\Delta,z)\,or\,u_0(x_\Delta)=\overline{u_0}(x_\Delta),$$
$$M_x(x_\Delta,z)=\overline{M_x}(x_\Delta,z)\,or\,w'^{(x_\Delta)}=\overline{w'}(x_\Delta),$$
$$M_\phi(x_\Delta,z)=\overline{M_\phi}(x_\Delta,z)\,or\,\phi(x_\Delta)=\bar{\phi}(x_\Delta), \quad (7)$$
$$M_{zz}(x_\Delta,z)=\overline{M_{zz}}(x_\Delta,z)\,or\,\psi(x_\Delta)=\bar{\psi}(x_\Delta),$$
$$V_z(x_\Delta,z)=\overline{V_z}(x_\Delta,z)\,or\,w(x_\Delta)=\bar{w}(x_\Delta).$$

Where

$$\begin{bmatrix} A \\ A_z \\ A_{zz} \end{bmatrix} = b\sum_{k=1}^{N}\int_{z_{(k-1)}}^{z_{(k)}} \begin{bmatrix} \overline{Q_{11}^{(k)}} \\ z\overline{Q_{11}^{(k)}} \\ z^2\overline{Q_{11}^{(k)}} \end{bmatrix} dz,$$

$$\begin{bmatrix} B \\ B_z \\ B_f \end{bmatrix} = b\sum_{k=1}^{N}\int_{z_{(k-1)}}^{z_{(k)}} \begin{bmatrix} f(z)\overline{Q_{11}^{(k)}} \\ zf(z)\overline{Q_{11}^{(k)}} \\ f(z)^2\overline{Q_{11}^{(k)}} \end{bmatrix} dz,$$

$$\begin{bmatrix} D \\ D_z \\ D_f \\ D_\phi \end{bmatrix} = b\sum_{k=1}^{N}\int_{z_{(k-1)}}^{z_{(k)}} \begin{bmatrix} \phi_{zz}^{(k)}(z)\overline{Q_{11}^{(k)}} \\ z\phi_{zz}^{(k)}(z)\overline{Q_{11}^{(k)}} \\ f(z)\phi_{zz}^{(k)}(z)\overline{Q_{11}^{(k)}} \\ \phi_{zz}^{(k)}(z)^2\overline{Q_{11}^{(k)}} \end{bmatrix} dz, \quad (8)$$

$$\begin{bmatrix} G \\ G_f \\ G_\beta \end{bmatrix} = b\sum_{k=1}^{N}\int_{z_{(k-1)}}^{z_{(k)}} \begin{bmatrix} \beta^{(k)}(z)f'(z)\overline{Q_{55}^{(k)}} \\ f'(z)^2\overline{Q_{11}^{(k)}} \\ \beta^{(k)}(z)^2\overline{Q_{11}^{(k)}} \end{bmatrix} dz,$$

$$\begin{bmatrix} \overline{N_x}(x_\Delta,z) \\ \overline{M_x}(x_\Delta,z) \\ \overline{M_\phi}(x_\Delta,z) \\ \overline{M_{zz}}(x_\Delta,z) \\ \overline{V_z}(x_\Delta,z) \end{bmatrix} = b\sum_{k=1}^{N}\int_{z_{(k-1)}}^{z_{(k)}} \begin{bmatrix} T_{x,} \\ zT_{x,} \\ f(z)T_{x,} \\ \phi_{zz}^{(k)}(z)T_{x,} \\ T_{z,} \end{bmatrix} dz.$$

2.4 Analytical solution

The Navier method was used to solve the differential equations, where the response fields are approximated using periodic functions. The boundary conditions for a simply supported beam are given by Eq. (9) and the solution is assumed to conform to Eq. (10).

$$\begin{aligned} w(0) = M_x(0,z) = M_{zz}(0,z) = M_\phi(0,z) = 0, \\ w(L) = M_x(L,z) = M_{zz}(L,z) = M_\phi(L,z) = 0. \end{aligned} \quad (9)$$

$$\begin{aligned} w(x) = \sum_{j=1}^{\infty} w_j sen\left(\frac{j\pi x}{L}\right), u_0(x) = \sum_{j=1}^{\infty} u_j cos\left(\frac{j\pi x}{L}\right), \\ \phi(x) = \sum_{j=1}^{\infty} \phi_j cos\left(\frac{j\pi x}{L}\right), \psi(x) = \sum_{j=1}^{\infty} \psi_j cos\left(\frac{j\pi x}{L}\right). \end{aligned} \quad (10)$$

3 Results and discussion

The results are presented in a dimensionless form according to Eq. (11) [19]. In this study, the shear stress field was obtained using equilibrium equations according to the procedure described by Reddy [20].

$$\begin{aligned} S = \frac{L}{2h},\ u_a^{(k)}(x,z) = \frac{u^{(k)}(x,z)E_y b}{2hq_0}, \\ \sigma_a^{(k)}(x,z) = \frac{\sigma^{(k)}(x,z)b}{q_0}, \tau_a^{(k)}(x,z) = \frac{\tau^{(k)}(x,z)b}{q_0}, \\ w_a(x) = \frac{w(x)800E_y bh^3}{L^4 q_0}. \end{aligned} \quad (11)$$

The following elastic properties were used for the fiber-reinforced laminated beam:

$$E_x = 25MPa, E_y = 1MPa, G_{xy} = 0.5MPa, G_{yz} = 0.2MPa,$$
$$v_{xy} = v_{yx} = 0.25.$$

The response fields (displacements and stresses) were analyzed for all higher-order beam theories adopted in this study (RED90, KRU49, SOL92, KAR03, and AKA07) in combination with the ZZ function proposed in this study (SIN-ZZ). The results obtained were compared with those of Vidal and Polit [18]. All analyses were performed for a simply supported beam subjected to sinusoidal load on surface $z = h$. The load is expressed as:

$$q(x) = \sum_{j=1}^{\infty} q_j sen\left(\frac{j\pi x}{L}\right) \text{ with } q_j = q_0(j=1). \quad (12)$$

The analytical solutions of the theory of elasticity developed by Pagano [19] were adopted as a reference.

3.1 Slenderness analysis (S Parameter)

The results of the displacement and stress fields were analyzed as the S parameter, Eq. (11), varied (from thick to thin) for a laminated composite beam formed by three layers of equal thickness and stacked in a 0°/90°/0° configuration. Tables 3–6 present, the maximum values and the relative error, for the transverse displacement, axial displacement, normal stress, and shear stress, respectively, obtained by Pagano [19], Vidal and Polit [18], and this study. Information in parentheses in tables refers to relative error. The results of the proposed method were obtained for different combinations of higher-order beam theories and ZZ-SIN function.

Given the combinations of the ZZ-SIN function and different higher-order kinematics, Tables 3–5 show minor relative errors for models SOL92, KRU49, and RED90 when the fields of axial displacement, transverse displacement,

Table 3 Maximum values for transverse displacement, $w(L/2)$

S	4	10	20	40
Ref. [19]	−2.8919	−0.9307	−0.6172	−0.5367
ZZ-SIN + RED90	−2.8624 (1.02%)	−0.9286 (0.19%)	0.617 (0.03%)	−0.5377 (0.19%)
ZZ-SIN + KRU49	−2.8624 (1.02%)	−0.9289 (0.19%)	−0.6174 (0.03%)	−0.5377 (0.19%)
ZZ-SIN + TOU91	−2.8470 (1.55%)	−0.9282 (0.27%)	−0.6173 (0.02%)	−0.5377 (0.19%)
ZZ-SIN + SOL92	−2.8636 (0.98%)	−0.9289 (0.19%)	−0.6174 (0.03%)	−0.5377 (0.19%)
ZZ-SIN + KAR03	−2.8285 (2.19%)	−0.9269 (0.41%)	−0.6171 (0.02%)	−0.5376 (0.18%)
ZZ-SIN +AKA07	−2.8280 (2.20%)	−0.9285 (0.24%)	−0.6174 (0.03%)	−0.5377 (0.19%)
Model [18]	−2.8026 (3.08%)	−0.9193 (1.22%)	−0.6151 (0.34%)	−0.5371 (0.07%)

Table 4 Maximum values for axial displacement, $u(L/h)$

S	4	10	20	40
Ref. [19]	−0.9330	−9.3487	−66.7796	−518.0090
ZZ-SIN + RED90	−0.9422 (0.99%)	−9.2800 (0.73%)	−66.7848 (0.007%)	−518.8415 (0.16%)
ZZ-SIN + KRU49	−0.9422 (0.99%)	−9.2800 (0.73%)	−66.7848 (0.007%)	−518.8415 (0.16%)
ZZ-SIN + TOU91	−0.9550 (2.36%)	−9.3216 (0.30%)	−67.5473 (1.15%)	−519.0181 (0.19%)
ZZ-SIN + SOL92	−0.9410 (0.89%)	−9.2761 (0.78%)	−66.7766 (0.004%)	−518.8250 (0.16%)
ZZ-SIN + KAR03	−0.9663 (3.57%)	−9.3594 (0.11%)	−66.9514 (0.26%)	−519.1788 (0.22%)
ZZ-SIN + AKA07	−0.9664 (3.58%)	−9.3090 (0.42%)	−66.8455 (0.098%)	−518.9645 (0.18%)
Model [18]	−0.9929 (6.32%)	−9.5434 (2.08%)	−67.3688 (0.88%)	−520.0402 (0.39%)

Table 5 Maximum values for normal stress, $\sigma(L/2, h)$

S	4	10	20	40
Ref. [19]	18.6791	73.6088	263.1913	1019.6630
ZZ-SIN + RED90	18.4999 (0.96%)	72.8850 (0.98%)	262.2633 (0.35%)	1018.7429 (0.09%)
ZZ-SIN + KRU49	18.4999 (0.96%)	72.8850 (0.98%)	262.2633 (0.35%)	1018.7429 (0.09%)
ZZ-SIN + TOU91	18.7510 (0.38%)	73.2120 (0.54%)	265.2575 (0.78%)	1019.0896 (0.06%)
ZZ-SIN + SOL92	18.4761 (1.09%)	72.8544 (1.02%)	262.2313 (0.36%)	1018.7106 (0.09%)
ZZ-SIN + KAR03	18.9745 (1.58%)	73.5086 (0.14%)	262.9174 (0.10%)	1019.4052 (0.03%)
ZZ-SIN + AKA07	18.9743 (1.58%)	73.1129 (0.67%)	262.5018 (0.26%)	1018.9843 (0.07%)
Model [18]	19.4954 (4.37%)	74.9538 (1.83%)	264.5566 (0.52%)	1021.0965 (0.14%)

Table 6 Maximum values for shear stress, $\tau(0,0)$

S	4	10	20	40
Ref. [19]	1.4299	4.2381	8.7493	17.6447
ZZ-SIN + RED90	1.4132 (1.17%)	4.2386 (0.01%)	8.7492 (0.01%)	17.6419 (0.02%)
ZZ-SIN + KRU49	1.4132 (1.17%)	4.2386 (0.01%)	8.7492 (0.01%)	17.6419 (0.02%)
ZZ-SIN + TOU91	1.4071 (1.59%)	4.2348 (0.08%)	9.0797 (3.77%)	17.6408 (0.02%)
ZZ-SIN + SOL92	1.4138 (1.13%)	4.2389 (0.02%)	8.7494 (0.01%)	17.6419 (0.02%)
ZZ-SIN + KAR03	1.4019 (1.96%)	4.2314 (0.16%)	8.7453 (0.05%)	17.6399 (0.03%)
ZZ-SIN + AKA07	1.4018 (1.97%)	4.2359 (0.05%)	8.7477 (0.02%)	17.6411 (0.02%)
Model [18]	1.4284 (0.10%)	4.2400 (0.04%)	8.7493 (0.00%)	17.6418 (0.02%)

and normal stress were analyzed. Regarding the analysis of the shear stress field (Table 6), SOL92, KRU49, RED90, and TOU91 resulted in lower relative errors among the combinations. As the S parameter increased, no significant change was observed in the relative errors for the combinations of ZZ-SIN and the higher-order beam theories. As shown in Tables 3–6, the ZZ-SIN+SOL92 combination had the lowest, or one of the lowest, values for the relative error. Tables 3–5 reveal that the ZZ-SIN+SOL92 combination presents significantly minor relative errors (error ≤ 1.09%) compared with the errors achieved by a previous model [18] (error ≤ 6.32%). For the shear stress field (Table 6), Vidal and Polit's approach [18] resulted in minor relative errors (error ≤ 0.10%) compared to the ZZ-SIN+SOL92 model (error ≤ 1.13%).

3.2 Analysis of number of layers

According to the results presented in Tables 3–6, the models of higher-order beams with the ZZ function (ZZ-SIN) exhibited significant differences in the results of the response fields of interest for thick beams ($S = 4$). It was observed that the SOL92 theory showed minor relative errors in most analyses, which justifies the study of the efficiency of the ZZ-SIN+SOL92 model in comparison with an alternative solution [18] as the number of layers is varied. Table 7 presents the stacking configuration for laminates with three, five, six, and eleven layers. In this analysis, the reference values are acquired from the theory of elasticity proposed by Pagano [19].

Table 7 Stacking-sequence terminology

N° layers	Stacking-sequence
3	$[0°/\overline{90°}]s$
5	$[0°/90°/\overline{0°}]s$
6	$[0°/90°/0°/90°/0°/90°]t$
11	$[0°/90°/0°/90°/0°/\overline{90°}]s$

The relative error of the maximum values and weighted average percentage error (WAPE) (shown in Eq. (13)) were used as metrics for the difference between the reference value, represented by X, and the calculated value, represented by x, either by the ZZ-SIN+SOL92 model or by that of Vidal and Polit [18].

$$W.A.P.E.(\%) = 100\frac{\sum_{j=1}^{n}\left|x_j - X_j\right|}{\sum_{j=1}^{n}\left|X_j\right|} \tag{13}$$

The results for the transverse displacement field, $w(x)$, measured using the WAPE metric along the longitudinal axis, and the relative error for the maximum value of the transverse displacement, $w(L/2)$, are presented in Table 8. Both the WAPE norm and the relative error for the maximum value of the transversal displacement have the same error percentage, with the ZZ-SIN+SOL92 model showing errors that are significantly lower than those of the model proposed by Vidal and Polit [18]. Moreover, with an increase in the number of layers, the errors of the previous model [18] tend to increase tremendously, whereas the model proposed remains almost stable at low values.

For the axial displacement field analysis, the WAPE norm was applied to the cross section at $x = L$, and the relative error for the maximum value was obtained at $x = L$ and $z = h$. As shown in Table 9, the ZZ-SIN+SOL92 model had a maximum error of 12.22%. For the model proposed by Vidal and Polit [18], the maximum error was 33.98% (both results were for a laminate with five layers).

Table 8 Maximum values and WAPE for transverse displacement

	$w(x)$			$w(L/2)$	
N° layer	ZZ-SIN + SOL92	Model [18]	Ref. [19]	ZZ-SIN + SOL92	Model [18]
3	0.98%	3.09%	−2.8919	−2.8636 (0.98%)	−2.8026 (3.08%)
5	1.25%	9.25%	−3.0516	−3.0135 (1.25%)	−2.7693 (9.25%)
6	2.08%	11.12%	−3.8492	−3.7689 (2.08%)	−3.4211 (11.12%)
11	0.86%	7.24%	−3.2184	−3.1908 (0.86%)	−2.9855 (7.24%)

Regardless of the number of layers, the ZZ-SIN+SOL92 model had a minor error compared with the other model [18], according to either the WAPE norm or the relative error for the maximum value of axial displacement. Analysis of the error referring to the maximum value of the axial displacement revealed that the ZZ-SIN+SOL92 model performed even better than that proposed by Vidal and Polit [18], as demonstrated by a maximum error of 1.77% for ZZ-SIN+SOL92 in comparison to the other model [18], which had a maximum error of 15.26%.

The analysis of the results in Tables 10 and 11 is similar to that discussed previously. For normal and shear stresses, the ZZ-SIN+SOL92 model had a minor error compared with the other model [18]. This performance was obtained by calculating the error for a given section (the WAPE metric) or the error for the maximum value of the shear stress or normal stress (relative error). Only for the value of maximum shear stress did the model proposed by Vidal and Polit [18] have better performance for laminates with three layers; however, when the number of layers increased, the ZZ-SIN+SOL92 model resulted in minor errors, with less influence of the number of layers compared with the previous model [18].

Table 9 Maximum values and WAPE for axial displacement

	$u(L, z)$			$u(L, h)$	
N° layer	ZZ-SIN + SOL92	Model [18]	Ref. [19]	ZZ-SIN + SOL92	Model [18]
3	7.42%	12.66%	−0.9330	−0.9410 (0.86%)	−0.9929 (6.32%)
5	12.22%	33.98%	−0.9360	−0.9526 (1.77%)	−1.0251 (9.51%)
6	9.53%	27.77%	−1.1742	−1.1645 (0.83%)	−1.3233 (15.26%)
11	5.92%	19.25%	−1.0247	−1.0212 (0.34%)	−1.1601 (13.21%)

Table 10 Maximum values and WAPE for normal stress

	$\sigma(L/2, z)$			$\sigma(L/2, h)$	
N° layer	ZZ-SIN + SOL92	Model [18]	Ref. [19]	ZZ-SIN + SOL92	Model [18]
3	5.65%	9.32%	18.6791	18.4761 (1.09%)	19.4954 (4.37%)
5	6.27%	17.41%	18.7379	18.7039 (0.18%)	20.1271 (7.41%)
6	6.82%	23.68%	23.4261	22.8642 (2.40%)	26.5724 (13.43%)
11	4.29%	18.04%	20.4828	20.0509 (2.11%)	22.7777 (11.20%)

Table 11 Maximum values and WAPE for shear stress

	$\tau(0, z)$			$\tau(0, 0)$	
N° layer	ZZ-SIN + SOL92	Model [18]	Ref. [19]	ZZ-SIN + SOL92	Model [18]
3	1.39%	1.41%	1.4299	1.4138 (1.13%)	1.4284 (0.10%)
5	1.51%	3.32%	1.6807	1.6729 (0.46%)	1.5244 (9.30%)
6	2.19%	11.73%	1.7501	1.7895 (2.25%)	1.5819 (9.61%)
11	0.90%	5.93%	1.6248	1.6397 (0.92%)	1.5030 (7.49%)

Figs. 3 and 4 show graphs for the variation in the response fields analyzed for a thick beam ($S = 4$) formed by five layers, according to the configuration shown in Table 7. Figs. 3(a) and 3(b) show graphs for the transverse displacement along the longitudinal axis and the axial displacement along the cross section at $x = L$. Figs. 4(a) and 4(b) show the normal stress field for the cross section at $x = L/2$ and the shear stress for the cross section at $x = 0$, respectively. Figs. 3 and 4 show that the ZZ-SIN+SOL92 model agrees better with the reference values for all the laminates. The Vidal and Polit model [18] resulted in significant discrepancies, mainly for the central laminate.

4 Conclusions

A higher-order ZZ function was coupled with several refined beam theories [3–8] to analyze laminated composite beams. The variation from thick to thin beams, represented by the S parameter, and the number and stacking of layers for a simply supported beam subjected to sinusoidal loading were analyzed to validate the proposed formulation. The results presented in Tables 3–6 show that higher-order beam theories influence the response fields when the beam is moderately to significantly thick. Furthermore, the ZZ-SIN+SOL92 model showed lower relative errors for most of the analyses as the S parameter varied, and with significantly better results than those of Vidal and Polit [18] were obtained when comparing with the reference values of Pagano [19].

For a thick laminated beam ($S = 4$), the amount and configuration of layer stacking influenced the analyzed response fields. According to both the WAPE norm and the relative error (the latter referring to the maximum value), the ZZ-SIN+SOL92 model presented significantly

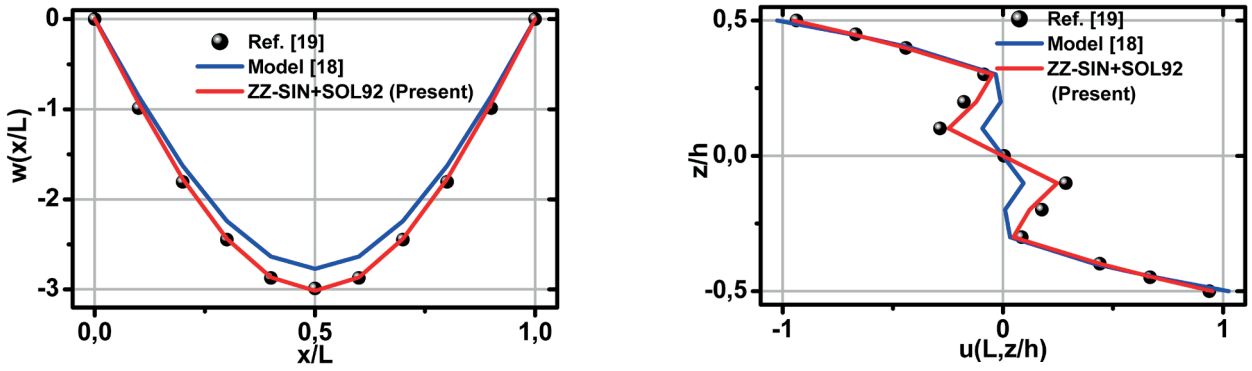

(a) (b)

Fig. 3 (a) Transverse displacement along the longitudinal axis and (b) axial displacement along the cross section at $x = L$, both for $S = 4$

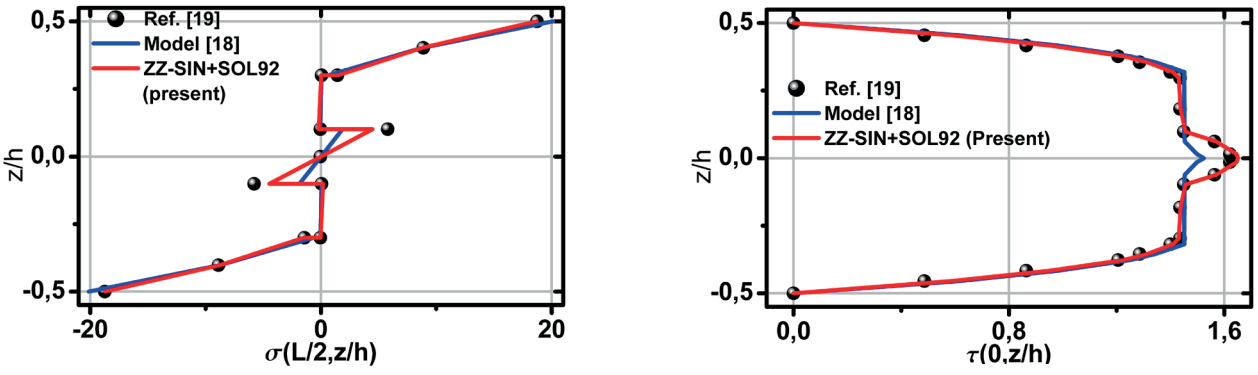

(a) (b)

Fig. 4 (a) Normal stress along the cross section at $x = L/2$ and (b) shear stress along the cross section at $x = 0$, both for $S = 4$

minor errors than those of the model proposed by Vidal and Polit [18], as shown in Tables 8–11. Moreover, the most significant discrepancies between the results of the analyzed models and the reference value occurred in the inner layers, as shown in Figs. 3 and 4 for a five-layer laminate.

Acknowledgments

This work was supported by the National Council for Scientific and Technological Development (CNPq), Process No. 402857/2021-6.

References

[1] Sayyad, A. S. "Comparison of various refined beam theories for the bending and free vibration analysis of thick beams", Applied and Computational Mechanics, 5(2), pp. 217–230, 2011. [online] Available at: https://www.kme.zcu.cz/acm/acm/article/view/161

[2] Timoshenko, S. P. "On the transverse vibrations of bars of uniform cross-section", The London, Edinburgh, and Dublin Philosophical Magazine and Journal of Science, 43(253), pp. 125–131, 1921. https://doi.org/10.1080/14786442208633855

[3] Kruszewski, E. T. "Effect of transverse shear and rotary inertia on the natural frequency of a uniform beam", [pdf] National Advisory Committee for Aeronautics, Langley Aeronautical Laboratory Langley Air Force Base, Washington, DC, USA, Technical Note 1909, 1949. Available at: https://ntrs.nasa.gov/citations/19930082587

[4] Reddy, J. N. "A general non-linear third order theory of plates with moderate thickness", International Journal of Non-Linear Mechanics, 25(6), pp. 677–686, 1990. https://doi.org/10.1016/0020-7462(90)90006-U

[5] Touratier, M. "An efficient standard plate theory", International Journal of Engineering Science, 29(8), pp. 901–916, 1991. https://doi.org/10.1016/0020-7225(91)90165-Y

[6] Soldatos, K. P. "A transverse shear deformation theory for homogeneous monoclinic plates", Acta Mechanica, 94(3), pp. 195–220, 1992. https://doi.org/10.1007/BF01176650

[7] Karama, M., Afaq, K. S., Mistou, S. "Mechanical behavior of laminated composite beam by the new multi-layered laminated composite structures model with transverse shear stress continuity", International Journal of Solids and Structures, 40(6), pp. 1525–1546, 2003. https://doi.org/10.1016/S0020-7683(02)00647-9

[8] Akavci, S. S. "Buckling and Free Vibration Analysis of Symmetric and Antisymmetric Laminated Composite Plates on an Elastic Foundation", Journal of Reinforced Plastics and Composites, 26(18), pp. 1907–1919, 2007. https://doi.org/10.1177/0731684407081766

[9] Vinson, J. R., Sierakowski, R. L. "The Behavior of Structures Composed of Composite Materials", Springer, 2008. ISBN: 978-1-4020-0904-4 https://doi.org/10.1007/0-306-48414-5

[10] Sayyad, A. S., Ghugal, Y. M. "Bending, buckling and free vibration of laminated composite and sandwich beams: A critical review of literature", Composite Structures, 171, pp. 486–504, 2017. https://doi.org/10.1016/j.compstruct.2017.03.053

[11] Murakami, H., Maewal, A., Hegemier, G. A. "A Mixture Theory with a Director for Linear Elastodynamics of Periodically Laminated Media", International Journal of Solids and Structures, 17(2), pp. 155–173, 1981. https://doi.org/10.1016/0020-7683(81)90072-X

[12] Di Sciuva, M. "A Refined Transverse Shear Deformation Theory for Multilayered Anisotropic Plates", Atti Accademia delle Scienze di Torino, 118, pp. 279– 295, 1984. (in Italian)

[13] Di Sciuva, M. "An Improved Shear-Deformation Theory for Moderately Thick Multilayered Anisotropic Shells and Plates", Journal of Applied Mechanics, 54(3), pp. 589–596, 1987. https://doi.org/10.1115/1.3173074

[14] Tessler, A., Di Sciuva, M., Gherlone, M. "A refined zigzag beam theory for composite and sandwich beams", Journal of Composite Materials, 43(9), pp. 1051–1081, 2009. https://doi.org/10.1177/0021998308097730

[15] Lularon, L., Gherlone, M., Di Sciuva, M., Tessler, A. "Assessment of the Refined Zigzag Theory for bending, vibration, and buckling of sandwich plates: a comparative study of different theories", Composite Structures, 106, pp. 777–792, 2013. https://doi.org/10.1016/j.compstruct.2013.07.019

[16] Carrera, E. "Historical review of Zig-Zag theories for multilayered plates and shells", Applied Mechanics Reviews, 56(3), pp. 287–308, 2003. https://doi.org/10.1115/1.1557614

[17] Carrera, E., Ciuffreda, A. "Bending of composited and sandwich plates subjected to localized lateral loadings: a comparison of various theories", Composite Structures, 68(2), pp. 185–202, 2005. https://doi.org/10.1016/j.compstruct.2004.03.013

[18] Vidal, P., Polit, O. "A sine finite element using a zig-zag function for the analysis of laminated composite beams", Composites Part B: Engineering, 42(6), pp. 1671–1682, 2011. https://doi.org/10.1016/j.compositesb.2011.03.012

[19] Pagano, N. J. "Exact solution for composite laminates in cylindrical bending", Journal of Composite Materials, 3(3), pp. 398–411, 1969. https://doi.org/10.1177/002199836900300304

[20] Reddy, J. N. "Mechanics of laminated composite plates and shells", CRC Press, 2004. eISBN: 9780429210693 https://doi.org/10.1201/b12409